NREL/TP-413-8008 • UC Category: 1263 • DE95009229

Novel Two-Stage Selenization Methods for Fabrication of Thin-Film CIS Cells and Submodules

Final Subcontract Report
1 March 1993 – 31 March 1995

B. Basol, V. Kapur, A. Halani,
C. Leidholm, A. Minnick
International Solar Electric Technology
Inglewood, California

NREL technical monitor: H. S. Ullal

National Renewable Energy Laboratory
1617 Cole Boulevard
Golden, Colorado 80401-3393
A national laboratory of the U.S. Department of Energy
Managed by Midwest Research Institute
for the U.S. Department of Energy
under contract No. DE-AC36-83CH10093

Prepared under Subcontract No. YI-2-12069-1

June 1995

NOTICE

Available to DOE and DOE contractors from:
Office of Scientific and Technical Information (OSTI)
P.O. Box 62
Oak Ridge, TN 37831
Prices available by calling (615) 576-8401

Available to the public from:
National Technical Information Service (NTIS)
U.S. Department of Commerce
5285 Port Royal Road
Springfield, VA 22161
(703) 487-4650

Printed on paper containing at least 50% wastepaper and 10% postconsumer waste

TABLE OF CONTENTS

LIST OF FIGURES

1.0 SUMMARY

This is the Phase II Final Technical Report of the subcontract titled "Novel Two-Stage Selenization Methods for Fabrication of Thin Film CIS Cells and Submodules." The general objectives of the program are the development of a cost-effective, large-area process for CIS film deposition, optimization of the various layers forming the CIS device structure, and fabrication of high efficiency submodules using these optimized device components. The specific goals of the project are the development of 10% efficient cells and 7% efficient submodules using a novel low cost CIS deposition approach, demonstration of 9% efficient submodules and 15% efficient cells using CIS layers obtained by the selenization of Cu-In metallic precursors.

During this research period, growth parameters of ZnO window layers were varied to optimize their electrical and optical properties. Using the MOCVD approach and boron (B) doping, ZnO films with resistivities in the low 10^{-3} Ω-cm range were grown at a substrate temperature of 175 °C. Investigation of the chemical interactions between the glass substrates, Mo layers and the selenization atmosphere revealed that the nature of the glass/Mo substrate greatly influenced the quality of the solar cells fabricated on them. Moderate amounts of sodium diffusing from the soda-lime glass substrate into the CIS film improved the efficiencies of the solar cells fabricated on such films . Mo layers allowing excessive Na diffusion through them, on the other hand, reacted excessively with the H_2Se environment and deteriorated the solar cell performance.

Addition of Ga into the CIS layers by the two-stage selenization technique yielded graded absorber structures with higher Ga content near the Mo/absorber interface. Cu-rich CIS layers were grown with grain sizes of larger than 5 μm. However, in-plane Cu_xSe phase separation in such layers did not allow efficient cell fabrication on these films even after the overall film stoichiometry was later adjusted to be In-rich.

In the Phase I Annual Report of this program large area CIS submodules with efficiencies of about 3% were reported. During the present Phase II program 1 ft^2 size CIS submodule efficiency was improved to 7%. Smaller area submodules with efficiencies as high as 9.79 % were also fabricated using CIS layers obtained by the H_2Se selenization method. The processing yield of the devices based on a non-vacuum CIS deposition approach was improved and solar cells with efficiencies greater than 10% were fabricated.

2.0 INTRODUCTION

This is the Phase II Final Technical Report of a subcontract titled "Novel Two-Stage Selenization Methods for Fabrication of Thin Film CIS Cells and Submodules." The objectives of this program are the development of a cost-effective, large-area process for CIS film deposition, optimization of various layers forming the CIS solar cell structure, and fabrication of efficient 1 ft^2 size CIS submodules using these approaches.

Recent advances made in CIS and related compound solar cell fabrication processes have clearly shown that these materials and device structures can yield power conversion efficiencies greater than 15%. Thin film CIS solar cells fabricated at ISET employing the two-stage selenization process have achieved conversion efficiencies of 13%. ISET's two-stage process for CIS thin film growth involves selenization of Cu-In precursors. In this approach the Mo coated glass substrate is first coated with a thin layer of Te. This step is then followed by the sequential deposition of In and Cu layers. The resulting films are highly alloyed Cu-In precursors that can be repeatably processed into good quality CIS layers. For CIGS absorber formation, Ga can be added into the precursor layer. The details of these processes and the results obtained were described in our 1992 Final Report [1] and will not be repeated here. The following sections of this report will provide information about three major areas of research carried out during the last 12-month period, i.e., investigation of the influence of the various cell components such as the glass substrate, the Mo contact and the ZnO window layer, on the performance of the CIS devices, large area submodule fabrication, and novel processing of CIS solar cells.

The specific goals of this program as listed in the "Statement of Work" and the "Schedule of Deliverables" are : The development of 10% efficient cells and 7% efficient submodules using a novel, non-vacuum CIS growth technique, and demonstration of 15% efficient cells and 9% efficient submodules using ISET's H_2Se selenization approach. Tasks performed during the last twelve months included ZnO layer optimization, optimization of the Mo contact layers, large area CIS processing and CIS film growth by a non-vacuum technique.

3.0 TECHNICAL DISCUSSION

Details of the selenization technique and the device fabrication steps employed in this program have been previously described [1, 2, 3]. In summary, Cu-In precursors of various stoichiometries were deposited onto Mo-coated soda-lime glass substrates at room temperature using the evaporation and sputtering methods. For the fabrication of small area films and devices and for specific experiments we used the e-beam evaporation approach. For large area substrates, the sputtering technique was employed. Gallium addition into the absorber layers was achieved by adding a thin layer of Ga into the Cu-In precursor stack. Selenization of the precursors was carried out in a reactor kept at a temperature of about 400 °C. The reactive atmosphere in the selenization chamber contained a mixture of H_2Se gas and Ar. For device fabrication, CIS films were coated with a thin (1000-2000 Å) CdS layer using the solution growth technique. This step was then followed by the deposition of a conductive ZnO window layer using the MOCVD method. For submodule fabrication monolithic integration steps were carried out as will be described in section 3.3.

3.1 Studies on Substrates and Contacts

During this research period work was carried out to correlate the CIS cell efficiency with the quality of the top and bottom contacts of the device.

3.1.1 Glass substrates and the Mo contact

Although, glass is commonly distinguished by its high chemical resistance at low temperatures, its reactivity may actually be extensive at temperatures employed in CIS film growth. The typical composition of a soda-lime glass sheet in weight percentages is 70% SiO_2, 15% Na_2O, and the balance, the oxides of Ca, Al, Mg, Ba and K [4]. The Na-O network in soda-lime glass is known to be reactive. Soda-lime glass, for example, leaches in acidic solutions through ion exchange which results in Na loss from the surface region. The glass surface also reacts with gases such as H_2, SO_2 and CO_2. These reactions may deplete the soda-lime glass surface of the alkali component if the reaction products are continuously removed from the surface.

Mo which is typically deposited on the glass substrates by the sputtering technique and it is the commonly used contact material in high efficiency CIS solar cells. Selection of Mo as the contact material to CIS is due to its relative stability under CIS film growth conditions. However, recent experience has shown that interaction of the glass/Mo substrate with the reactive CIS growth environment can be substantial especially in a selenization process involving H_2Se.

In this work Mo films were grown on various types of glass substrates in a sputtering system with vertical geometry. The substrates were passed in front of a DC magnetron cathode at a controlled speed to deposit 1-3 μm thick layers. Soda-lime glass with 14%Na_2O, Corning 7740 glass containing 4% Na_2O , and Na-free Corning 7059 glass samples were used as the substrates. Deposition parameters such as the background pressure, sputtering gas pressure, cathode-to-substrate distance and sputtering power level were changed and the resulting films were evaluated as for their stress, thickness and resistivity. Witness samples of 50 μm thick borosilicate glass were used to determine the type of intrinsic stress (compressive vs. tensile) in the films by evaluating the curvature of these substrates after Mo depositions.

Plain, glass samples and Mo/glass structures were selenized in a H_2Se atmosphere at around 400 °C for about 30 minutes. Auger depth profiling was used to determine the degree of selenization near the surface regions of the Mo layers deposited on different types of glass substrates. XPS measurements were employed to investigate the reaction products on the Mo surfaces. Two-point resistance measurements were used to compare the resistive Mo surfaces formed after the selenization step. The measurement involved placement of two probes on the selenized Mo surfaces separated by a distance of about 1 cm. All of the experiments mentioned above were repeated on soda-lime glass samples coated with a 3000 Å thick evaporated SiO_2 film.

After the selenization step a visual inspection of the various glass samples showed that the soda-lime glass surface was covered with a thin layer of reaction products. The surfaces of all the other glasses including the soda-lime sheet with the SiO_2 barrier layer were totally clear of any residues or reaction products. The reacted glass surface changed color to light brown when it was exposed to air and cooled to below 100 °C. Viewing under the microscope, one could observe that the surface layer absorbed moisture from the air forming small nodules.

The explanation for the observed phenomenon lies in the reaction of sodium on the surface of the soda-lime glass substrate with the H_2Se atmosphere at 400 °C following the reaction:

$$Na_2O(s) + H_2Se(g) \text{ ----- } Na_2Se(s) + H_2O(g)$$

which is favorable. Na_2Se is a deliquescent material and therefore it readily absorbs water vapor from air when taken out of the reaction chamber and cooled to below 100 °C. Resulting species are expected to be NaOH and Se precipitates.

Diffusion of Na from the glass substrate into the CIS layers grown by the co-evaporation technique has been previously reported and the influence of this diffusion process on the device efficiency has been discussed [5]. It should be noted that the results of the experiment described above is specific to the H_2Se selenization technique. In selenization approaches using elemental Se as the source material, reaction of Na_2O with Se vapor is

not as favorable. In fact, we have not observed any reaction products on soda-lime glass substrates selenized with Se vapor in a vacuum chamber using Se evaporation. It is, therefore, important to distinguish between the selenization approaches while addressing the issue of glass reactivity.

After confirming the reactivity of Na in soda lime glass substrates with the H_2Se atmosphere, we carried out experiments to study the possible influence of this behavior on the Mo/glass structures and solar cells.

The relationships between the micro-structure and stress of Mo films and the sputtering conditions employed for the deposition of such layers have been well established [6]. Overall, the Mo layers obtained at low sputtering gas pressures tend to be dense and low-resistivity and they are under compressional stress due to the atomic peening process. As the Ar gas pressure is increased, film stress switches from compressional to tensile. Further increases in the working pressure may yield stress-free layers with porous micro-structures. The electrical resistivities of such layers may be orders of magnitude higher than the bulk resistivity ($5.5x10^{-6}$ ohm-cm) of Mo depending upon the residual oxygen pressure in the sputtering chamber. A sketch qualitatively showing the relationships between the Mo film characteristics and the sputtering process parameters is shown in Fig. 1. This data was obtained from ISET's Mo sputtering process and it follows the trends observed by others. It should be noted that although the general behavior of the pressure-stress curves in the Mo sputtering process is well understood, the absolute values of the

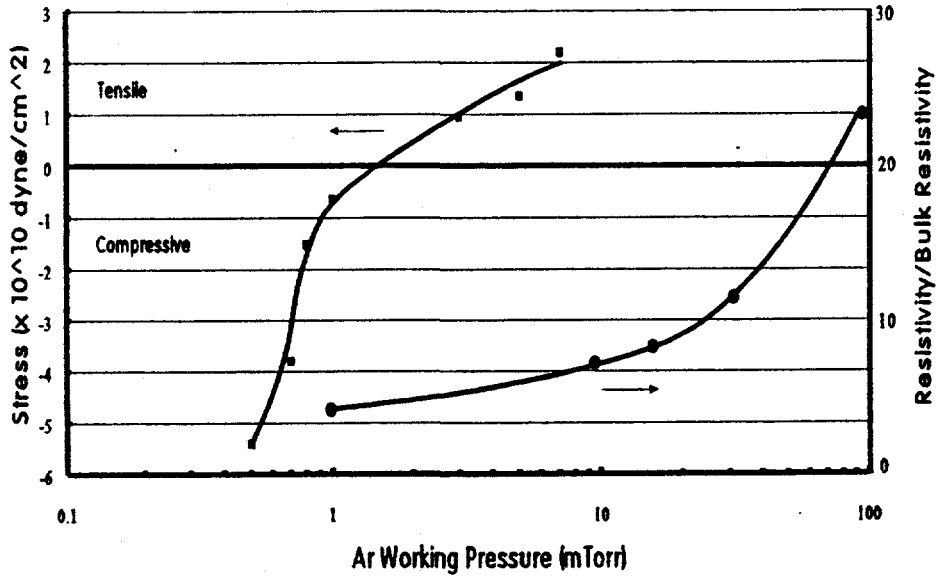

Fig. 1 ISET's sputtered Mo film characteristics as a function of Ar pressure. Background pressure was $1x10^{-6}$ Torr, power was 2.2 kW on a 5"x15" target.

Ar gas pressures where the stress transition from compressional to tensile occurs may change from system to system because the film structure is also influenced by other factors such as the system geometry, ion bombardment of the substrate, deposition angles, substrate temperature and sputtering voltage/power etc.

The above mentioned structural and electrical properties of sputtered Mo layers play an important role in determining certain characteristics of the glass/Mo substrates and solar cells fabricated on them. Adhesion of the Mo film to the glass surface and the sheet resistance of the solar cell back contact are two factors that need to be taken into consideration. However, we should not forget that the sputter deposited Mo film is not used in the cell structure in its as-deposited form. Rather, it goes through the processing steps necessary for the fabrication of a complete device including a high temperature selenization step. Therefore, its properties measured right after deposition may not necessarily be the same as they are in the finished device structure.

The Auger surveys and depth profiles obtained from two different Mo layers that were selenized at 400 °C are given in Figs. 2a and 2b. These films were both deposited on soda-lime glass substrates. In Fig. 2a, the data taken from sample Mo-60 display about four times the Na signal observed at the surface of Mo-127. There is also a larger O signal.

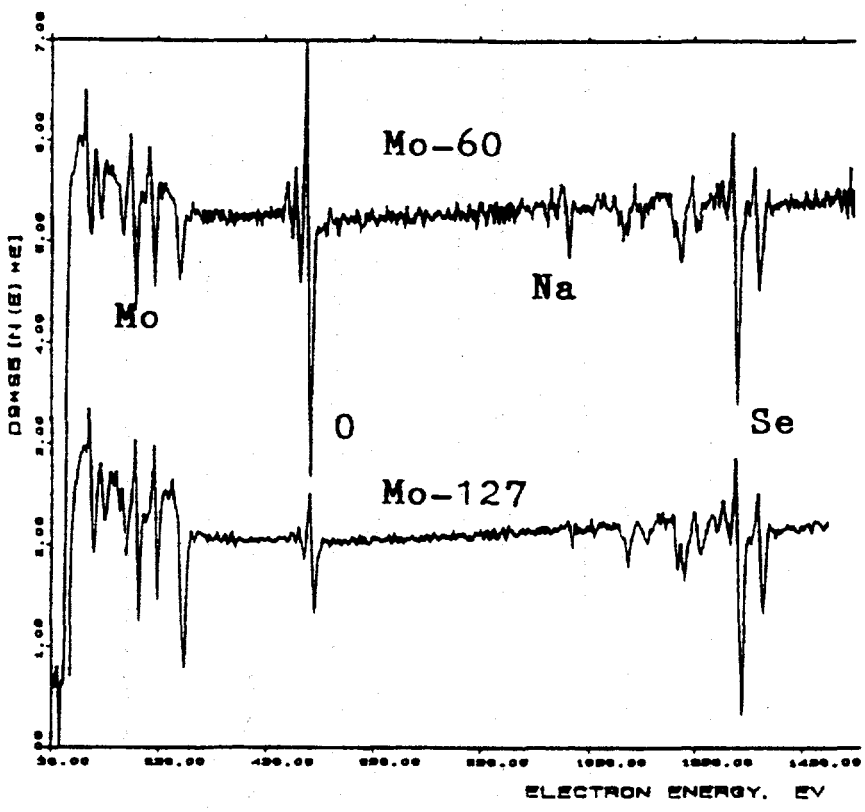

Fig. 2a Auger survey spectra of the Mo-60 and Mo-127 sample surfaces.

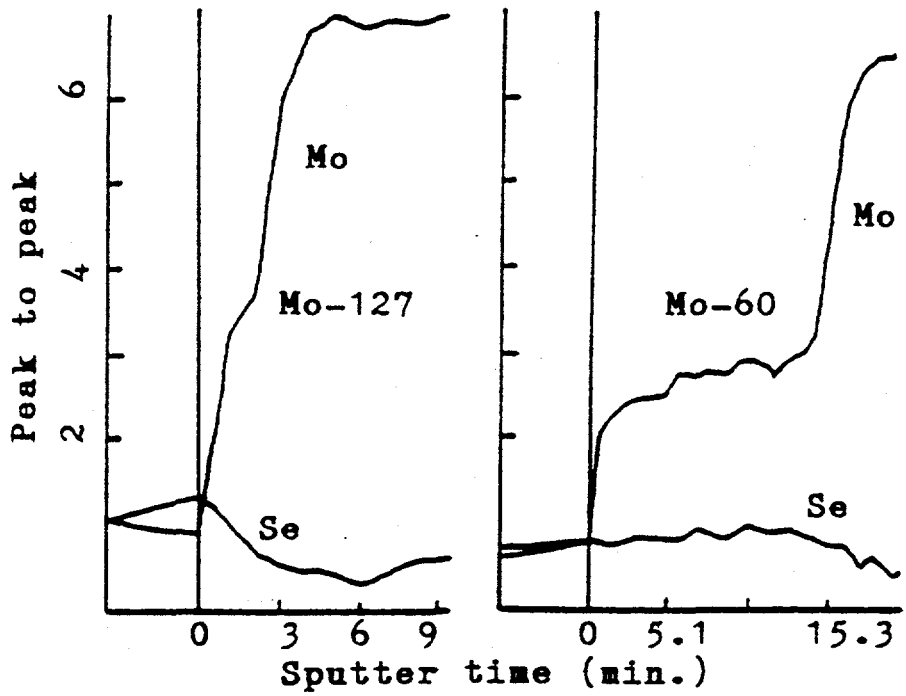

Fig. 2b Auger depth profiles of the Mo-60 and Mo-127 samples.

Auger depth profiles shown in Fig. 2b suggest that Mo-127 has a thin layer of selenide (about 1500 Å) on its surface, whereas, the selenized surface of Mo-60 is about five times thicker. It should be noted that Mo-60 film had a dark powdery layer on its surface that could be wiped off. After removing this layer both the Na and the O peaks observed in AES survey were reduced, however, they still were stronger than those for sample Mo-127. Two-point resistance measurements made on the two selenized Mo films indicated resistance values of 2-10 Kohms for Mo-60 and 10-300 ohms for Mo-127. The XPS survey spectra of the two Mo films are shown in Fig. 3a. This data indicates about five times more Na on the surface of Mo-60 compared with Mo-127. The Mo 3d spectra of the two samples (Fig. 3b) show the double peaks associated with $MoSe_2$. However, in the spectra of Mo-60 there is clearly a third peak shifted by 3.8 eV that can be attributed to Na_2MoO_4. The Se 3d spectra of Fig. 3c display the expected $MoSe_2$ peak for both samples. The data of Sample Mo-60, however, has additional peaks shifted by 4.6 eV (Na_2SeO_3 and/or SeO_2) and 8.9 eV (possibly higher order Se oxides).

All the results discussed above point to the fact that two different Mo layers on the same soda-lime glass substrate may selenize differently. Excessive reaction of Mo with the selenizing atmosphere yields a dull surface layer with high resistivity which is associated with the appearance of a strong Na signal as observed from the Auger as well as the XPS data presented above. Therefore, reactivity of the Mo surface is related to Na diffusion from the glass substrate to the Mo surface region. The degree of Na diffusion, on the other

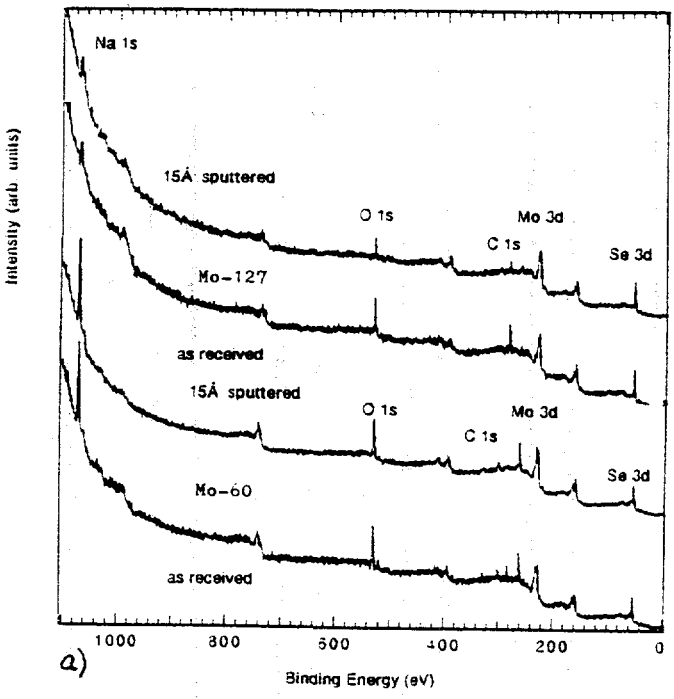

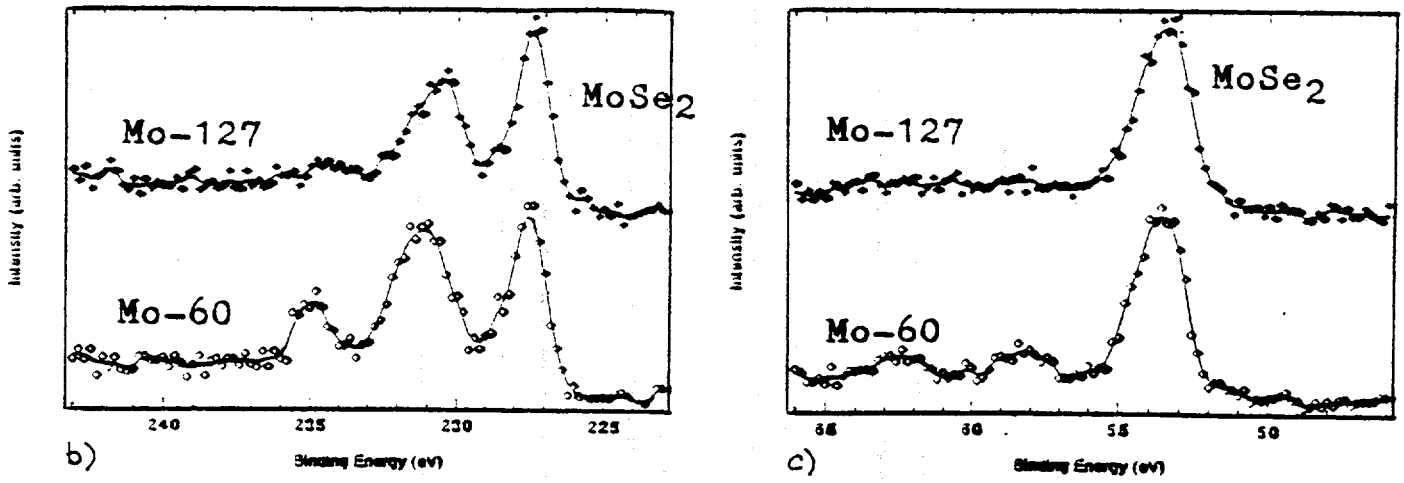

Fig. 3 a) XPS survey spectra, b) Mo 3d and c) Se 3d spectra taken from samples Mo-60 and Mo-127.

hand, depends on the nature of the Mo film itself.

To further correlate the surface reactivity of Mo film with Na diffusion, the selenization experiments were repeated on glass/Mo samples using glass sheets of various compositions. Mo films equivalent to sample Mo-60 did not show excessive reaction with the selenizing atmosphere when they were deposited on Corning 7044 and Corning 7059 glass substrates. Similarly, excessive reaction was not observed for Mo layers deposited on soda lime glass substrates with a surface barrier layer of 3000 Å thick SiO_2.

Effect of the excessive reaction between the selenizing atmosphere and the Mo surface on CIS cell performance was studied in an experiment on two solar cells fabricated on soda-lime glass/Mo substrates. The Mo layer of the first device had developed a thick surface layer when selenized separately. Two- point resistance measurement gave a value of 8 K ohms for this Mo sample after selenization. The Mo layer of the second device, on the other hand, was equivalent to the Mo-127 sample of Fig. 2. The Cu-In precursors and all the details of CIS film and device processing steps were identical for the two solar cells. The illuminated I-V characteristics of the devices showed that the cell fabricated on the reactive Mo layer suffered from a poor fill factor value that can be attributed to the presence of a high resistivity region at the Mo/CIS interface.

The above example demonstrated the deleterious effect of excessive Na diffusion through the Mo layer on the cell characteristics. Na diffusion into the CIS film at moderate levels, however, can improve the device efficiency as shown in Fig. 4. This figure shows the illuminated I-V characteristics of a set of devices fabricated on soda-lime (A), Corning 7740 (B) and Corning 7059 (C) glass substrates. Device D was prepared on a soda-lime glass substrate with a SiO_2 surface barrier layer between the glass surface and the Mo contact. The experiment was carried out using CIS layers with Cu/In ratios of 0.88, 0.92 and 0.98. The general observations from the data of Fig. 4 and the other experiments can be listed as follows:

i) The efficiency of the solar cell fabricated on the soda-lime glass substrate (without the SiO_2 barrier layer) was higher than those fabricated on other glass substrates.

ii) The difference between the efficiencies of the soda-lime-glass-based device and the others was the largest for the lowest Cu/In ratio. For devices employing CIS layers with Cu/In ratios of 0.92 and 0.98 the differences between the fill factor values of various cells were not as dramatic as they are in Fig. 4.

iii) A thin layer of SiO_2 deposited on the soda-lime glass surface before Mo deposition lowered the fill factor of the CIS cells.

The above results suggest that Na diffusing through the Mo layer into the CIS film dopes the CIS layer. Consequently, good devices can be obtained at low Cu/In ratios with Na

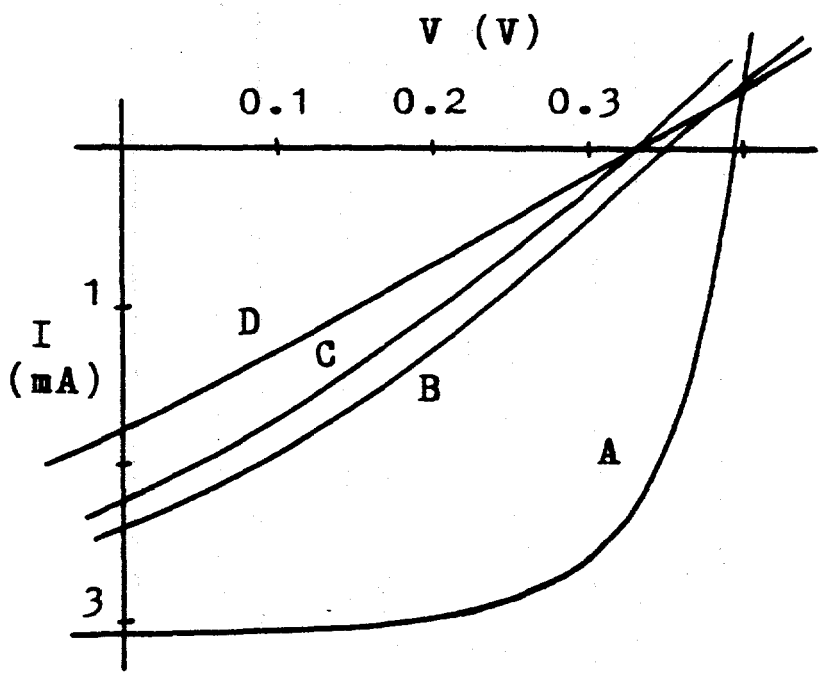

Fig. 4 Illuminated I-V characteristics of 0.09 cm^2 CIS cells fabricated on soda-lime glass (A), Corning 7740 glass (B), Corning 7059 glass (C), and soda-lime glass coated with SiO_2 (D). The Cu/In ratio for the CIS film was 0.88.

doping. Presence of Na actually increases the processing window of solar cells in terms of usable CIS stoichiometric ratios.

3.1.2 ZnO window layers

One of the tasks of this project was the optimization of the ZnO window layer. During this period we carried out a study of the ZnO MOCVD deposition process with the aim of fine-tuning its variables. These variables included the substrate temperature, flow rates of the reactants and the dopant concentration. The deposition technique involved reaction of water vapor with diethylzinc (DEZ) on substrates heated to a temperature range of 150-200 °C. Doping was achieved by diborane gas addition into the reactant flow. Deposition was done at a pressure range of 0.8-2 Torrs. Sheet resistance and optical transmission of the resultant films were measured and evaluated.

A typical set of resistivity vs. substrate temperature data is shown in Fig. 5 for various amounts of diborane in the reactant flow. It is clear that the electrical properties of the MOCVD grown ZnO films depend very strongly on the substrate temperature, and for this set of samples it shows a distinct minimum at a substrate temperature of 175 °C. It is also

interesting to observe that the minimum resistivity point does not change appreciably with the B dopant concentration. The sharp variation in the resistivity of MOCVD grown ZnO with the substrate temperature originates from the changes in the electron mobilities of the films as has been previously studied by other groups [7]. Initially, the crystalline size and the electron effective mobility of the material increase with increasing substrate temperature. At substrate temperatures of higher than 175 °C, however, crystalline structure of the material becomes disordered and the mobility values decrease along with the resistivity values. Increasing the diborane flow rate decreases the resistivity initially. This decrease, however, saturates at high B concentrations. Highly doped layers also display increased optical absorption at long wavelengths due to free carrier absorption. Presently we are using ZnO films with resistivity values of around $1x10^{-3}$ Ω-cm deposited at a substrate temperature of 175 °C.

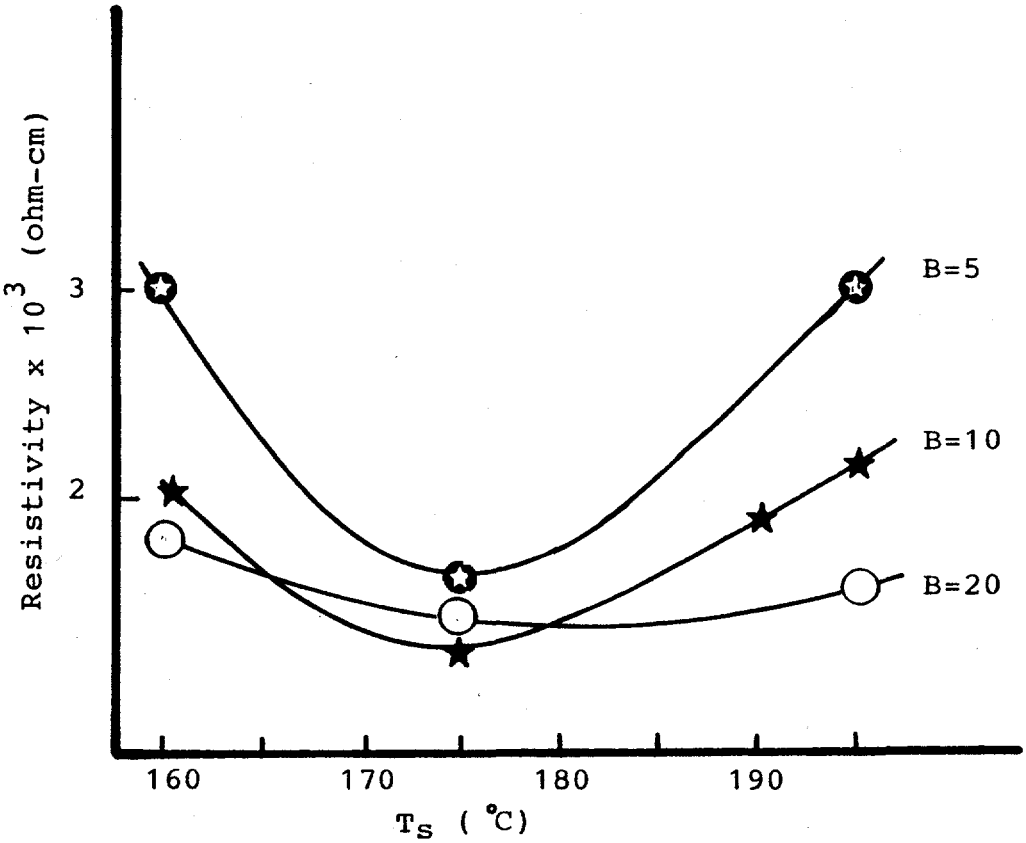

Fig. 5 Relationship between the resistivity and the substrate temperature for MOCVD grown ZnO layers. Dopant concentrations are given in relative units.

3.2 Studies on Absorber Layers

One approach used by various research groups to improve the quality of co-evaporated CIS absorber layers is to bring the overall stoichiometry of the film into the Cu-rich region for a period of time and then to adjust it back to the In-rich composition which is required for high efficiency device fabrication. Such an approach is known to improve the grain size of the resulting films because of the fluxing action of the CuSe phase present in the Cu-rich layers grown under Se-rich conditions. We had previously applied this technique to the CIS layers prepared by the H_2Se selenization method by dividing the CIS growth process into two steps, the first one to grow a Cu-rich bottom layer, and the second to grow an In-rich CIS film on top of the first layer [8]. During this period a more systematic study was carried out to asses the feasibility of adjusting the stoichiometry of Cu-rich CIS layers obtained by the selenization technique. Another topic of investigation was the addition of Ga into the CIS absorber layers.

3.2.1 Cu-rich CIS films

According to the Cu_2Se-In_2Se_3 pseudo binary phase diagram, the homogeneity region of single phase CIS extends from the stoichiometric composition of 50 mole% In_2Se_3 to the In-rich composition of about 55 mole % In_2Se_3 [9]. The corresponding Cu/In ratio for the single phase material is between 1.0 and 0.82. According to the same phase diagram, CIS films with Cu/In ratios of greater than 1.0 are expected to contain the secondary phase of Cu_2Se which is a highly conducting material with resistivities in the 10^{-2} ohm-cm range.

The SEM of Fig. 6 demonstrates the influence of a high Cu/In stoichiometric ratio on the structure and chemical composition of a CIS layer which was obtained by selenizing an e-beam evaporated Cu-In precursor at a temperature of 500 °C for 15 minutes. The Cu/In ratio in the precursor of this layer was adjusted to around 1.2 by controlling the total thicknesses of the evaporated In and Cu films. The cross sectional SEM of this film showed a dense layer of 1-2 μm size columnar grains. The lower magnification surface view of the same film, on the other hand, indicates that there is a high aerial density of much larger grains of 5-10 μm size which are imbedded in the matrix of this compact structure (Fig. 6). The compositions of the large grains as well as that of the smaller grains were analyzed by Energy Dispersive X-ray Analysis (EDAX) which indicated that while the smaller grain matrix basically consisted of the near-stoichiometric CIS phase, the large grains were almost totally depleted of In. In other words, selenization of a Cu-rich Cu-In precursor film at 500 °C yielded a CIS+Cu_2Se layer with segregated Cu_2Se grains. When selenization experiments were carried out on the same Cu-rich precursor at 450 °C, similar results were obtained. However, the overall grain size of the resulting film was smaller. Films with higher Cu/In ratios had grain sizes as high as 10 μm but these layers were discontinuous. An example of a layer with Cu/In ratio of 1.8 is shown in Fig. 7.

The grain growth observed in Cu-rich CIS films is believed to result from the fluxing action

of CuSe phase which has a low melting point of around 525 °C. It should be noted that CIS films obtained from the selenization of precursors with Cu/In ratios in the 0.85-0.9 range typically yield 0.2-1.0 μm size grains and no phase segregation.

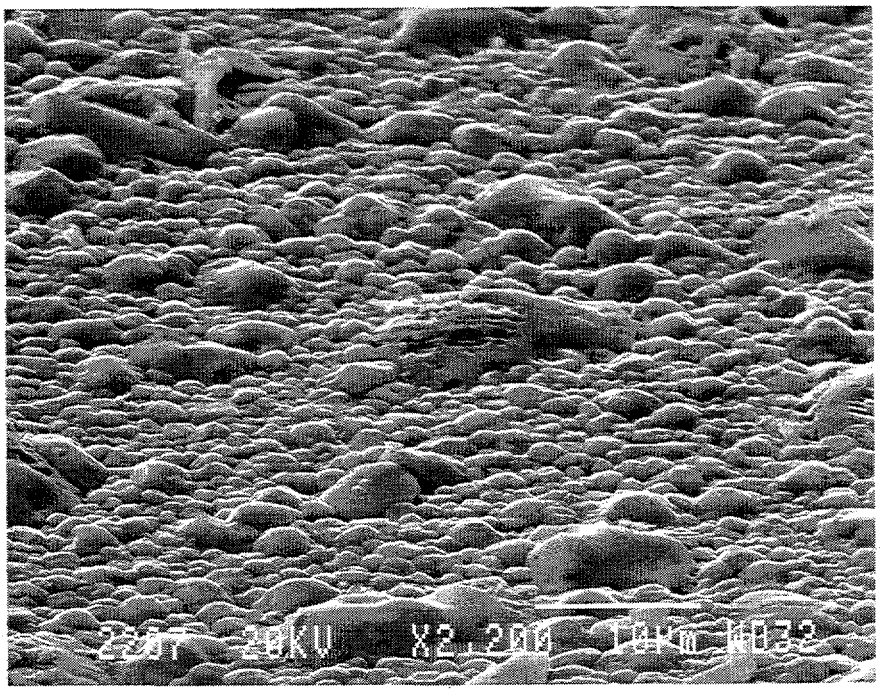

Fig. 6 SEM of a Cu-rich CIS film with Cu/In ratio of 1.2. The protruding large grains observed in the SEM were found to be Cu_2Se-rich.

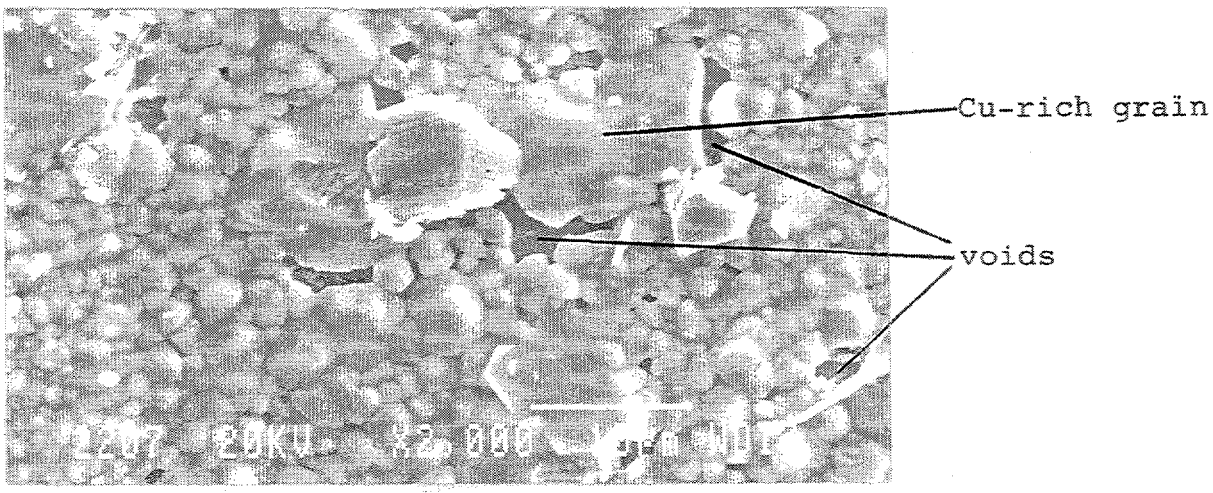

Fig. 7 SEM of a CIS+Cu_2Se film with Cu/In ratio of 1.8.

Cu_2Se phase segregation in Cu-rich films is expected from the Cu_2Se-In_2Se_3 phase diagram. However, the extent and the form of separation depends on the nature of the film growth technique. For example, in the Cu-rich films obtained by the elemental co-evaporation process the Cu_2Se phase was reported to segregate to the surface areas of the single phase CIS grains during the early stages of deposition. As the thickness of the evaporated film increased, the CIS grains merged together to form a compact columnar structure and the Cu_2Se phase totally segregated to the surface of the growing film [10]. This "vertical segregation" of Cu_2Se phase in co-evaporated Cu-rich CIS films is depicted in Fig. 8a. It should be noted that the Cu-rich surface in such films can be eliminated by increasing the flux of the evaporated In towards the end of the deposition process. In fact, this is a commonly used approach for growing good quality In-rich CIS films. In the co-evaporation technique the composition of the evaporated flux is continuously adjusted from highly Cu-rich to highly In-rich during the growth period. CIS films prepared by this approach display the large grain size of a Cu-rich material with the desirable electronic properties of an In-rich composition.

The SEM of Fig. 6b points to a different form of Cu_2Se phase separation in the Cu-rich films prepared by our selenization process. This "in-plane segregation" phenomena may be due to the high mobilities of species during the reaction step of the process and it gives rise to total separation of Cu_2Se grains throughout the selenized film as depicted in Fig. 8b. It should be appreciated that such an in-plane stoichiometric non-uniformity in a selenized layer can not be eliminated by reacting this film further with additional In. Therefore, the processing approach described above for the growth of large grain CIS films by the co-evaporation technique can not be readily applied to the selenization method. The technique could be applied to CIS layers with lower Cu content ($1<Cu/In<1.2$) reacted at lower temperatures ($400°C<T<500°C$).

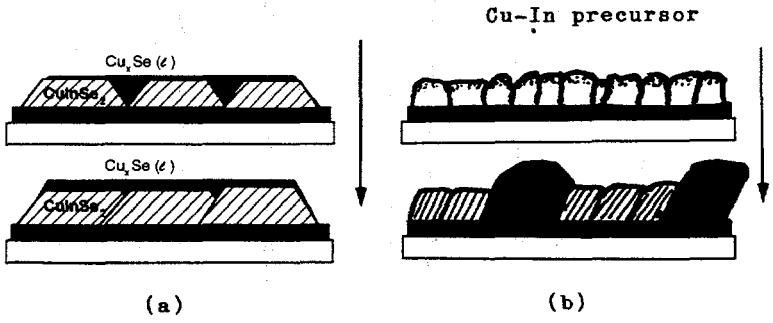

Fig. 8 Evolution of Cu_2Se phase separation in a) co-evaporated Cu-rich CIS films (ref. 10), b) Cu-rich layers prepared by the selenization technique.

3.2.2 Films containing Ga

During this research period work was carried out to grow CIGS absorber layers by adding Ga into the metallic precursors. Gallium was deposited at the bottom, middle or top of the Cu-In precursor stacks before their selenization. Experiments were carried out with Ga amounts corresponding to 10-25 atomic percent in the final film (with respect to Ga+In). For each case studied, irrespective of the original position of the Ga layer in the metallic precursor, Ga was found to segregate next to the Mo/absorber interface after the reaction in the H_2Se atmosphere . An example of this phenomenon can be seen in the data of Fig. 9. Figure 9a is the Auger depth profile of a Cu-In metallic precursor film containing Ga near its surface. The Auger depth profile of the same film after the selenization step is shown in Fig. 9b. The Ga signal in this case was found to peak at the back of the device structure indicating segregation of Ga-rich phases. Attempts to obtain uniform CIGS layers by the low temperature H_2Se selenization technique were not successful. Apparently, the kinetics or thermodynamics of the reactions favor only CIS formation close to the solid-gas interface at the temperatures employed. It is possible that at higher temperatures of > 500 °C under certain conditions one may get uniform CIGS layers by the selenization technique. However, such high temperatures are detrimental to the mechanical integrity of the Mo contact layers, especially in selenization processes using highly reactive H_2Se gas.

Although the H_2Se selenization has been unable to produce uniform CIGS films to date, the graded structures that it naturally yields are desirable for device fabrication. Presence of larger bandgap CIGS compounds near the contact interface of the CIS device is expected to form a back surface field which can help current collection, especially if the absorber thickness is reduced. We have fabricated cells with active area efficiencies in the 11-13% range using 1 μm thick graded CIGS layers obtained by H_2Se selenization.

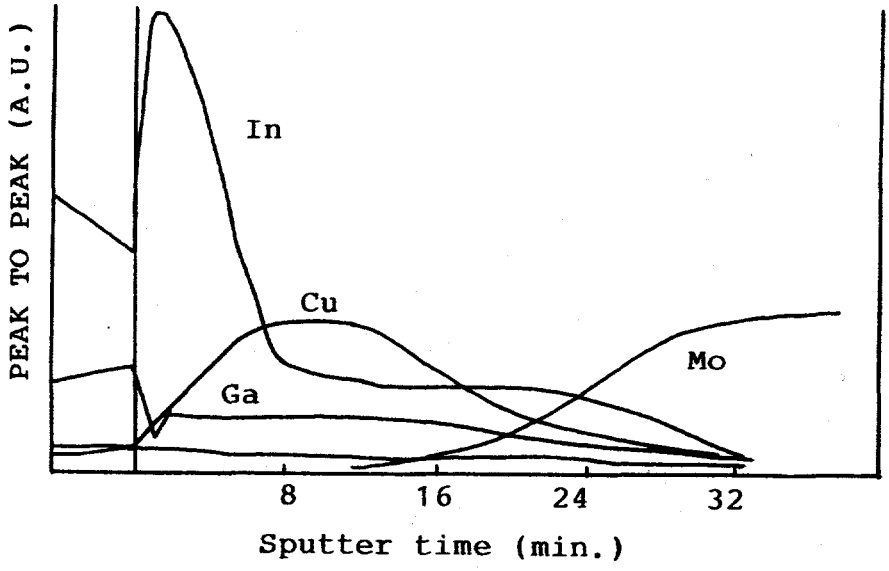

Fig. 9a Auger depth profile of a precursor prepared for selenization.

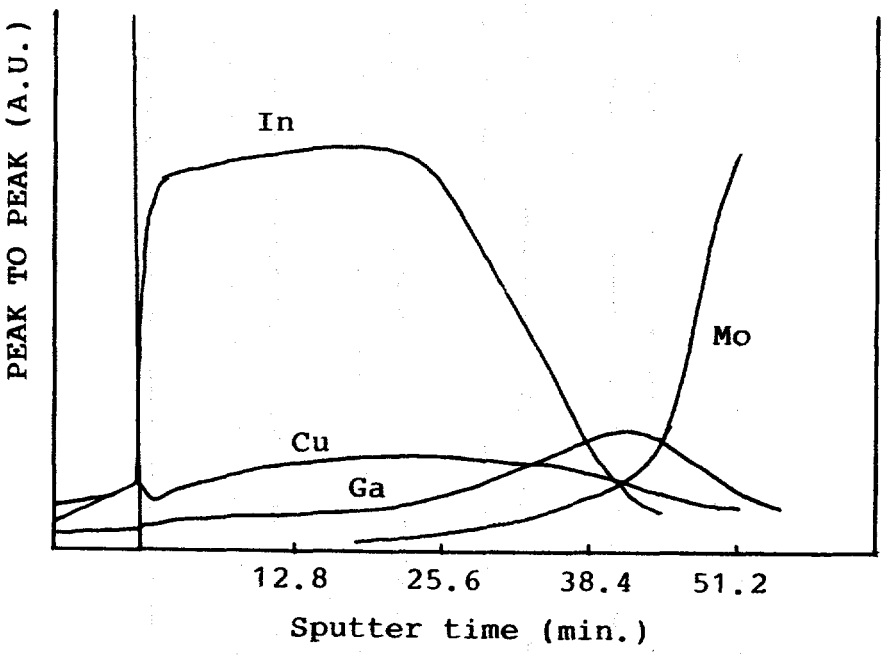

Fig. 9b Auger depth profile of the film obtained by selenizing the film of Fig. 9a at around 400 °C in a H_2Se atmosphere.

3.3 Submodule Fabrication

Mo, Cu and In depositions on large area glass substrates were carried out in a sputtering chamber. The substrates were vertically mounted in the substrate carrier which allowed the substrates to be passed in front of the cathodes at a constant speed. Both the substrate's speed and its distance to the targets were adjustable. Film thicknesses were controlled by adjusting the cathode power, sputtering pressure, substrate-to-target distance, and the speed of the substrate. Relationship between the cathode power level and the coating thickness at a given pressure was found to be linear [1].

Achieving uniform Cu/in ratios over 1 ft^2 size glass substrates requires fine-tuning the sputtering conditions and developing the proper shielding for cathodes that would produce uniform Cu and In film thicknesses throughout the substrate. By mapping the film thicknesses and adjusting the shape of the cathode shields we were able to improve thickness uniformities of Cu and In films and hence improve the stoichiometric uniformity of the CIS films. However, we should point out that control of the run-to-run stoichiometric uniformity of the precursor layers is an important issue to be resolved. A deposition approach with feedback loop control based on stoichiometry is needed for improving the yields of CIS module fabrication through an in-line process.

For submodule fabrication, Cu-In precursors were deposited on scribed glass/Mo substrates and then the films were selenized and processed through the monolithic integration steps described before [1]. In summary, a 1000-2000 Å thick layer of CdS was first deposited on the CIS layer using the solution growth method. A 2-3 mil wide channel was then scribed in the composite film to expose the Mo contact along the edges of the Mo segments. A layer of doped ZnO was applied by the MOCVD technique to form the top electrode and to make the electrical connection, through the scribes, with the lower Mo contacts. Module integration was completed by making a final isolation scribe through the ZnO/CdS/CIS layers. Both of these scribes were made using a computer controlled mechanical scriber which was designed and built during this Phase II program. Figure 10 illustrates an integrated section of a typical CIS submodule. The total width of individual cells in this design is in the range of 0.52-0.555 cm.

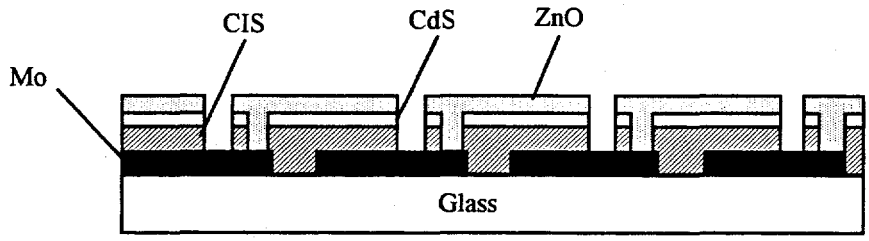

Fig. 10 A section of the integrated CIS submodule showing the interconnection approach.

Modules with sizes ranging from 15 cm^2 to 900 cm^2 were fabricated using the above mentioned procedures. The illuminated I-V characteristics for one of the nominally 1 ft^2 size CIS submodule measured at NREL is given in Fig. 11.

The device of Fig. 11 had an aperture area 845 cm^2. There were 55 cells in series, each about 0.52 cm wide. The photovoltaic parameters of this submodule were; V_{oc} = 22.62 V, J_{sc} = 0.5474 mA/cm^2, FF = 55.53%, P_{max} = 5811.1 mW and EFF = 6.88 %. The open circuit voltage value corresponds to 0.41 V per cell which is about the same as we reported at the end of Phase I program. The short circuit current density at the cell level is 30.11 mA/cm^2 a big improvement over the 23 mA/cm^2 value that was previously reported for the 4% efficient submodules of Phase I. We have fabricated several of such submodules and

measured efficiencies in the range of 6-7 % at ISET. Area loss due to scribes in this group of devices was about 7%. The spectral response measurements indicated rather low response at long wavelength that was attributed to ZnO absorption. This submodule was also characterized at NREL using the laser scanner setup. Results indicated that two of the 55 cells making up this device had very low output. Further analysis indicated that these cells were shorted due to mechanical defects. Laser scanner also indicated that there was a region of about 1.0-1.5 inch width at the top and bottom of the submodule that yielded low output. These edges were parallel to the direction of travel of the substrate during Cu and In depositions. These results correlated well with our atomic absorption spectroscopy measurements on similar devices which indicated stoichiometric non-uniformities in the areas of low output.

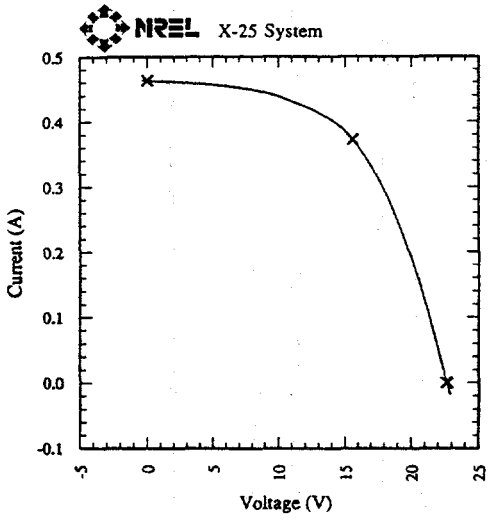

V_{oc} = 22.62 V
I_{sc} = 0.4626 A
J_{sc} = 0.5474 mAcm^{-2}
Fill Factor = 55.53 %

V_{max} = 15.60 V
I_{max} = 0.3724 A
P_{max} = 5811.1 mW
Efficiency = 6.88 %

Fig. 11 Illuminated I-V characteristics of a CIS submodule measured at NREL.

Smaller size submodules were also fabricated during this period on absorber layers with better stoichiometric uniformities. The I-V characteristics of two such devices measured at ISET are given in Fig. 12. These devices utilized absorber layers containing about 20% Ga in a graded structure described before in this report. One of the submodules had an aperture area of 58.25 cm^2. It consisted of 25 cells in series. The parameters of the I-V data given in Fig. 12 are V_{oc} = 11.47 V (0.459 V per cell), J_{sc} = 1.36 mA/cm^2, and FF = 60.52 %. The aperture area efficiency can be calculated to be 9.1 % for this device. The second submodule of Fig. 12 had an area of 139 cm^2 with V_{oc} = 11.26 V (25 cells in series), J_{sc} = 1.28 mA/cm^2, FF = 56.71% and EFF = 8.14%. Voltage per cell is 0.45 V. It should be noted that the high voltages can be more repeatably obtained from cells employing a graded absorber structure than those fabricated on CIS layers.

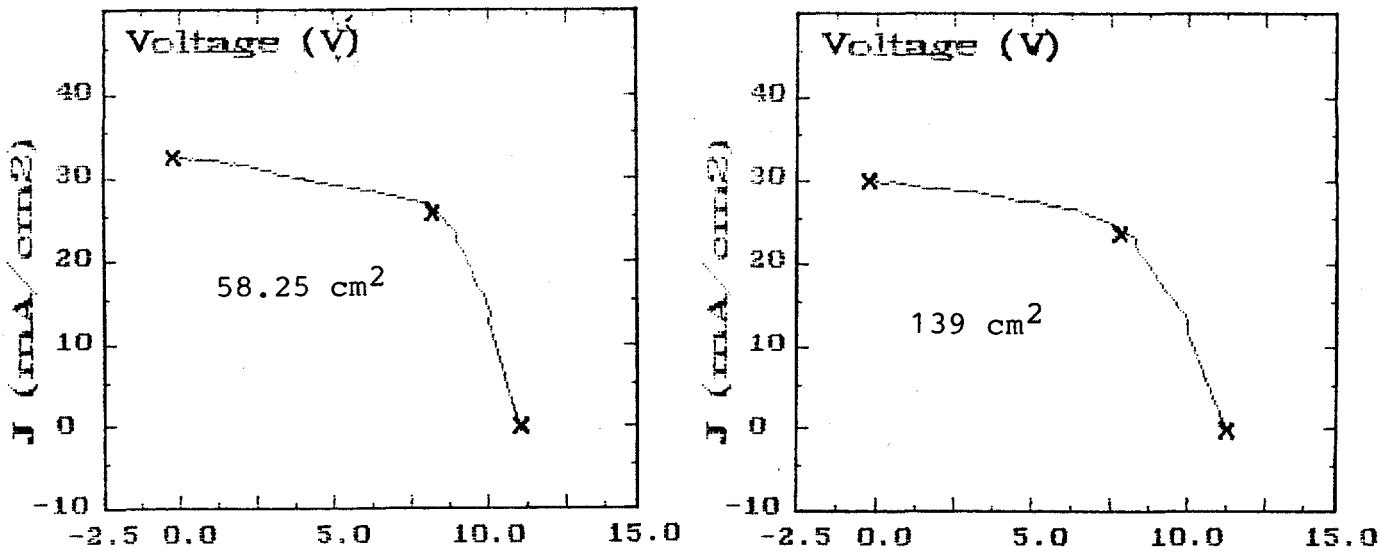

Fig. 12 I-V characteristics of two submodules measured at ISET.

The I-V characteristics and the relative quantum efficiency of a 144.9 cm^2 submodule measured at NREL are given in Fig. 13. The efficiency of this device is 9.79% under AM1.5 illumination. There were 20 cells in series, each about 0.55 cm wide. The open circuit voltage per cell is 0.472 V. Relatively poor red response observed in the spectral response data is due to absorption in the ZnO layer which was about 3 μm thick for this device. At that thickness the sheet resistance obtained was around 3-5 ohms/square.

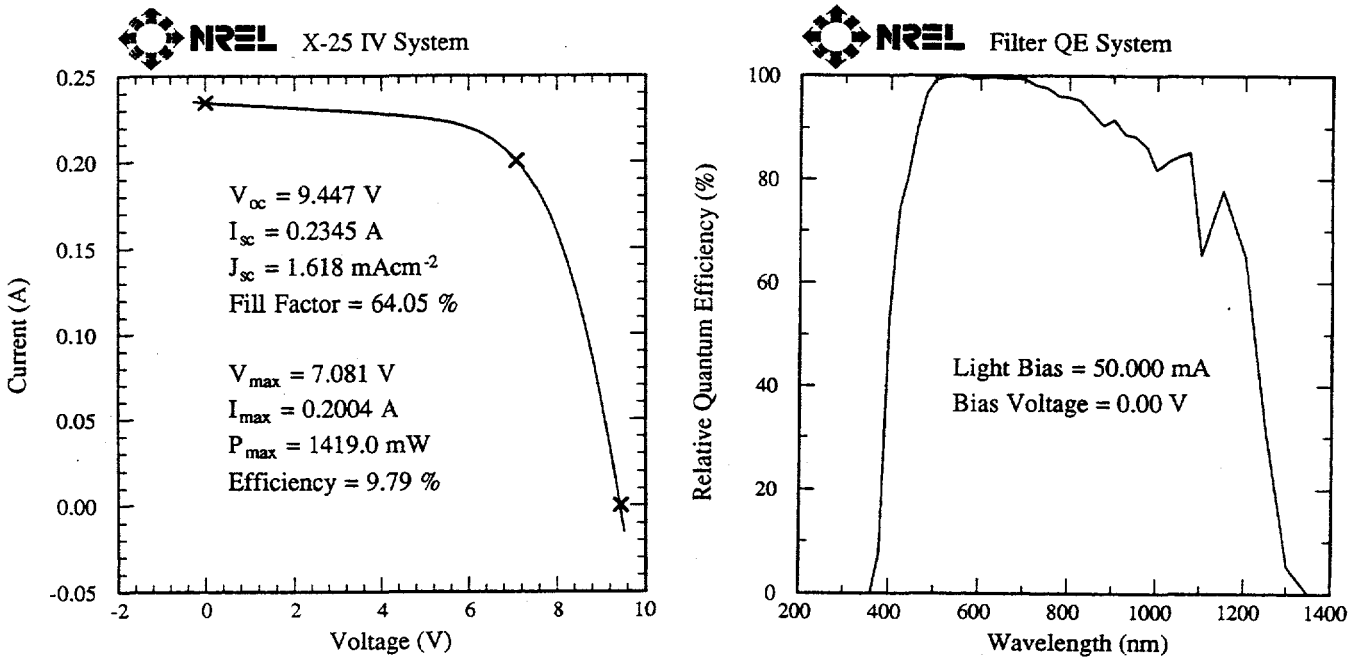

Fig. 13 The IV characteristics (a) and the quantum efficiency (b) of an ISET submodule fabricated on a CIGS layer.

3.4 Novel CIS Deposition Method

A primary concern in establishing CIS module manufacturing is the cost of capital equipment. In processes using vacuum techniques, this can be substantially high. Therefore, investigation into alternative methods of solar cell fabrication exhibiting both low capital costs and low manufacturing costs are of great interest.

In Phase I of this contract we identified and performed research on a novel non-vacuum CIS film deposition technique which has the potential of having very low manufacturing costs. In Phase II, we developed this technique further and improved the device efficiencies and yield. We also fabricated first submodules using this technique.

One of the most attractive features of the novel technique is that it uses established current-technology processes for device fabrication. A device structure used in many vacuum-based processes, namely glass/Mo/CIS/CdS/ZnO configuration, is also employed here. However, the formation of the CIS absorber layer is done by a non-vacuum process.

The device efficiencies have steadily improved as a better understanding of the process is achieved. The device efficiencies in Phase I project were as high as 10%. However, the yield was not very good and the scatter of the efficiency values was high, many cells being fabricated with efficiencies in the 5-10% range. During the Phase II program optimization work was done to improve the yield . As a result, the average efficiency of cells was improved and a great number of devices with efficiencies in the 7-11% range were fabricated. The I-V characteristics of a device with about 11% efficiency is given in Fig. 14. The solar cell parameters of this device with 0.09 cm^2 area are; V_{oc} = 0.42 V, J_{sc} = 39 mA/cm^2 and FF = 67.1%. This cell used a thin ZnO layer to minimize absorption losses in this window film.

In addition to discrete cell fabrication, work was also initiated to fabricate integrated modules by the novel technique. The result of an early attempt using monolithic integration steps of section 3.3 is shown in Fig. 15. The aperture efficiency of this eight-cell submodule is 4.5%. In depth study of this device indicated that the monolithic integration steps used for the sputtered/selenized CIS devices could not be directly applied to the non-vacuum processing approach because the nucleation and growth of the material on the scribed regions of the Mo layer are very different in the two approaches. Films prepared on scribed Mo layers by the novel ISET approach give rise to shorting paths along the Mo scribe lines. ISET will be working on this issue and develop an integration scheme that can be used with its novel technology.

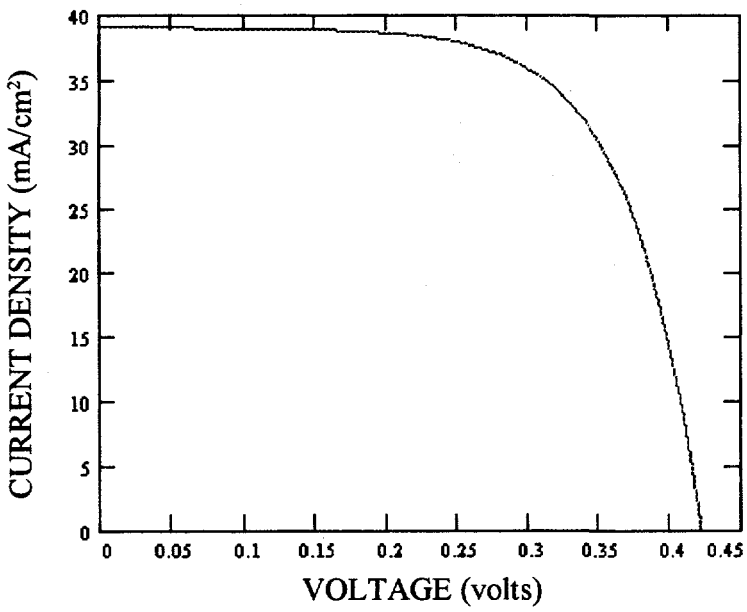

Sample: R612A

V_{oc} = 0.420 volts
J_{sc} = 39.0 mA/cm²
Fill Factor = 67.1 %
Efficiency = 11.0 %

I_{sc} = 3.51 mA
P_{max} = 0.990 mW
I_{max} = 3.09 mA
V_{max} = 0.320 volts

Fig. 14 I-V characteristics of a cell fabricated on a CIS layer obtained by ISET's novel technique.

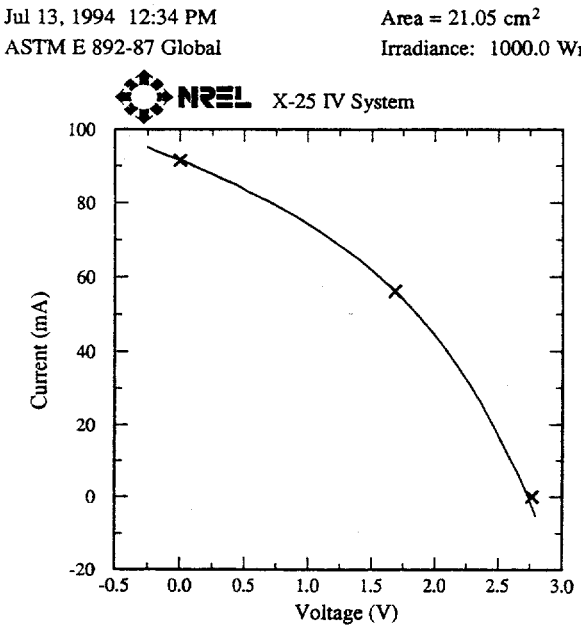

V_{oc} = 2.765 V
I_{sc} = 91.45 mA
J_{sc} = 4.345 mAcm⁻²
Fill Factor = 37.43 %

V_{max} = 1.684 V
I_{max} = 56.18 mA
P_{max} = 94.63 mW
Efficiency = 4.50 %

Fig. 15 A monolithically integrated submodule fabricated on a CIS layer obtained by ISET's novel technique.

4.0 CONCLUSIONS

During this Phase II program there have been several accomplishments to improve ISET's thin film CIS photovoltaics technology. Specifically, the module fabrication process was streamlined and completed by the addition of a computer controlled mechanical scriber. This piece of hardware can handle up to 1 ft^2 size substrates and it was designed and built by ISET. Better stoichiometric control over large area substrates and more optimized module processing steps led to the improvement of 1 ft^2 size submodule efficiencies which increased from about 4% to about 7% during this Phase II program. Smaller size submodules were also fabricated with efficiencies as high as 9.79 %. ISET's new non-vacuum CIS deposition technique which had yielded over 10% efficient devices during Phase I program was further developed during this Phase II period. The most important improvement was in the yield of this process in terms of its capability of producing over 9% efficient cells in a repeatable manner. The best devices made by this technique during the present research period were about 11% efficient using CIS absorbers.

5.0 ACKNOWLEDGMENTS

The authors are grateful to R. Matson, A. Swartzlander-Franz, A. Nelson, A. Mason and K. Emery of NREL for measurements of films and devices and to H. Ullal, R. Noufi and K. Zweibel for extensive technical discussions.

6.0 LIST OF PUBLICATIONS

During the last 12 month period the following publications were published on the subject of thin film solar:

- B.M. Başol, V.K. Kapur, A. Halani, A. Minnick and C.R. Leidholm, "Modules and flexible cells of CIS", Proc. 23rd IEEE PVSC, 1993, p. 426.

- B.M. Başol, "Preparation techniques for thin film solar cell materials", Jpn. J. Appl. Phys., 32 (1993) 35.

- B.M. Başol, V.K. Kapur, C.R. Leidholm, A. Minnick and A. Halani, "Development of low-cost thin film CIS cells and modules", 12th NREL PV Program Rev., AIP Conf. Ser. 306, 1994, p. 79.

- B.M. Başol and V.K. Kapur, "Processing of CIS films for photovoltaics", Mat. Res. Soc. Symp. Proc. vol. 327, 1994, p. 71.

- V.K. Kapur, B.M. Başol, A. Halani C.R. Leidholm and A. Minnick, "Technical and business factors affecting commercialization of thin film CIS technology", 12th European PVSEC, 1994, p. 1608.

- B.M. Başol, V.K. Kapur, C.R. Leidholm, A. Minnick and A. Halani, "Studies on substrates and contacts for CIS films and devices", Proc. 1st World Conf. PVEC, 1994, in press.

7.0 REFERENCES

1. B.M. Başol, V.K. Kapur, A. Halani and C. Leidholm, "Low cost CIS submodule development", Final Subcontract Report, July 7, 1990-January 31, 1992, NREL/TP-413-5010.
2. B.M. Başol and V.K. Kapur, 21st IEEE PVSC, 1990, p. 546.
3. B.M. Başol, V.K. Kapur and R.J. Matson, 22nd IEEE PVSC, 1991, p. 1179.
4. R. Brown in "Handbook of thin film technology" eds.L. Maissel and R. Glang, McGraw Hill, 1970, p. 6-8.
5. M. Bodegard, L. Stolt and J. Hedström, 12th European PVSEC, 1994, p. 1743.
6. J.A. Thornton in "Deposition Technologies for Films and Coatings" eds. R.F. Bunshah et al., Noyes , 1982, p. 170.
7. W.W. Wenas, A. Yamada and K. Takahashi, J. Appl. Phys., 70 (1991) 7119.
8. B.M. Başol, V.K. Kapur and R.C. Kullberg, Solar Cells, 27 (1989) 299.
9. M.L. Fearheiley, Solar Cells, 16 (1986) 91.
10. J. Tuttle, M. Contreras, A. Tennant, D. Albin and R. Noufi, 23rd IEEE PVSC, 1993, p. 426.

REPORT DOCUMENTATION PAGE

Form Approved
OMB NO. 0704-0188

1. AGENCY USE ONLY (Leave blank)	2. REPORT DATE	3. REPORT TYPE AND DATES COVERED
	June 1995	Final Subcontract Report, 1 March 1993 - 31 March 1995

4. TITLE AND SUBTITLE

Novel Two-Stage Selenization Methods for Fabrication of Thin-Film CIS Cells and Submodules

5. FUNDING NUMBERS

C: YI-2-12069-1

TA: PV531101

6. AUTHOR(S)

B. Basol, V. Kapur, A. Halani, C. Leidholm, A. Minnick

7. PERFORMING ORGANIZATION NAME(S) AND ADDRESS(ES)

International Solar Electric Technology
8635 Aviation Blvd.
Ingelwood, CA 90301

8. PERFORMING ORGANIZATION REPORT NUMBER

9. SPONSORING/MONITORING AGENCY NAME(S) AND ADDRESS(ES)

National Renewable Energy Laboratory
1617 Cole Blvd.
Golden, CO 80401-3393

10. SPONSORING/MONITORING AGENCY REPORT NUMBER

TP-413-8008

DE95009229

11. SUPPLEMENTARY NOTES

NREL Technical Monitor: H. S. Ullal

12a. DISTRIBUTION/AVAILABILITY STATEMENT

12b. DISTRIBUTION CODE

UC-1263

13. ABSTRACT *(Maximum 200 words)*

This report describes several accomplishments to improve International Solar Electric Technology's (ISET's) thin-film $CuInSe_2$ (CIS) photovoltaics (PV) technology. Specifically, the module fabrication process was streamlined and completed by adding a computer-controlled mechanical scriber. This piece of hardware can handle up to 1-ft^2 substrates, and it was designed and built by ISET. Better stoichiometric control over large-area substrates and more-optimized module processing steps led to the improvement of 1-ft^2 submodule efficiencies, which increased from about 4% to about 7% during this program. Smaller submodules were also fabricated with efficiencies as high as 9.79%. ISET's new non-vacuum CIS deposition technique, which yielded more than 10%-efficient devices during Phase 1, was further developed during Phase II. The most important improvement was in the yield of this process in terms of its capability of producing greater than 9%-efficient cells in a repeatable manner. The best devices made by this technique were about 11% efficient using CIS absorbers.

14. SUBJECT TERMS

selenization ; fabrication ; thin films ; copper indium diselenide ; submodules ; photovoltaics ; solar cells

15. NUMBER OF PAGES
28

16. PRICE CODE

17. SECURITY CLASSIFICATION OF REPORT	18. SECURITY CLASSIFICATION OF THIS PAGE	19. SECURITY CLASSIFICATION OF ABSTRACT	20. LIMITATION OF ABSTRACT
Unclassified	Unclassified	Unclassified	UL